A Novel Frequency-Domain Implementation of Tomlinson-Harashima Precoding for SC-FDMA

Mohamed Noune and Andrew Nix
Centre for Communications Research, University of Bristol
Merchants Ventures Building, Woodland Road, BS8 1TJ, Bristol UK
Email: {Mohamed.Noune,Andy.Nix}@bristol.ac.uk

***Abstract*— There is considerable interest in the use of Single Carrier Frequency Division Multiple Access (SC-FDMA) as the uplink transmission scheme in the 3GPP Long Term Evolution standard. This interest is justified by the inherent single carrier structure of SC-FDMA, which results in reduced sensitivity to phase noise and a lower Peak-to-Average Power Ratio (PAPR) compared to Orthogonal Frequency Division Multiple Access. This, consequently, makes it more attractive for low cost devices with limited transmit power. In this paper we demonstrate how precoding the uplink transmission is an alternative signal processing technique to equalization in order to combat the frequency selective nature of the propagation channel. The frequency-domain implementation of Tomlinson-Harashima Precoding (THP) for uplink SC-FDMA is proposed. We investigate the BER performance and the PAPR characteristics of the precoded SC-FDMA waveform for ZF and MMSE based THP. Results reported here show that the MMSE-THP outperforms the ZF-THP in terms of BER performance and PAPR.**

***Index Terms*: 3GPP LTE, SC-FDMA, Tomlinson-Harashima Precoding, PAPR, Equalization.**

I. Introduction

THE significant expansion seen in mobile and cellular technology over the last two decades is a direct result of the increasing demand for high data rate transmissions over bandwidth and power limited wireless channels. This requirement for high data rates results in significant inter-symbol interference (ISI) for single carrier systems, and this requires the use of robust coding and powerful signal processing techniques in order to overcome the time and frequency selective natures of the propagation channel. Orthogonal Frequency Division Multiplexing (OFDM) has been proposed for a range of future standards. Particular examples include the physical layer of high performance Wireless Local Area Networks (WLANs), such as the 802.11 family of standards [1]- [2]. This trend has occurred since OFDM offers high performance and low terminal complexity. For short range devices, despite the high peak-to-average power ratio (PAPR) of the OFDM signal [1], these solutions are more common than their single carrier counterparts.

The Third Generation Partnership Project (3GPP) Long Term Evolution (LTE) radio access standard is based on shared channel access providing peak data rates of 75 Mbps in the uplink and 300 Mbps in the downlink. A working assumption in the LTE standard is the use of Orthogonal Frequency Division Multiple Access (OFDMA). This is used to support different carrier bandwidths (1.25–20 MHz) in both Frequency Division Duplex (FDD) and Time Division Duplex (TDD) modes [3]. OFDMA is an OFDM-based multiple access scheme [1] that provides each user with a unique fraction of the system bandwidth. It is highly suitable for broadband wireless networks due to the advantages it offers, including scalability, robustness to multipath and MIMO compatibility [2]. On the other hand, OFDMA is very sensitive to frequency offset and phase noise, which requires accurate frequency and phase synchronization [1]. In addition, OFDMA is characterized by a high PAPR, which results in reduced mean power and coverage for the low cost power amplifiers used at the handset. For these reasons, OFDMA is not well suited for uplink transmissions. To address these issues, SC-FDMA has been proposed for use on the uplink of the LTE standard [3].

Given its inherent single carrier structure, SC-FDMA can be considered as an extension of Single-Carrier Frequency Domain Equalization (SC-FDE) [4], with a flexibility in resource allocation. SC-FDMA can be used with a range of single carrier Frequency Domain Equalization (FDE) techniques to combat the frequency selective nature of the transmission channel. These include frequency-domain Linear Equalization (LE), Decision Feedback Equalization (DFE) and the more recent Turbo Equalization [5]. Frequency-domain LE is analogous to time-domain LE. A Zero-Forcing (ZF) based LE eliminates the ISI completely but degrades the system performance due to noise enhancement. Superior performance can be achieved by using the Minimum Mean Square Error (MMSE) criterion. Decision Feedback Equalization (DFE) offers a performance that is superior to that of conventional LE because of its ability to cancel precursor echoes without noise enhancement. These equalizers are required to produce instantaneous decisions. When incorrect decisions are made, DFEs behave poorly due to error propagation. In order to overcome these shortcomings, alternative schemes have been proposed. These include the block-based DFE [6], the Frequency Domain Equalizer with Noise Prediction [7]- [8] and Tomlinson-Harashima Precoding (THP) [9]- [10].

THP is an effective way to account for the error propagation problem in a DFE since its feedback filter is implemented at the transmitter and is thus error free [9]- [10]. Since precoding does not suffer from error propagation, precoding can be combined with coded modulation schemes such as Trellis precoding [11], precoding for noise whitening on ISI channels [12] and precoding for partial-channel response [13]. THP, which was originally proposed to combat intersymbol interference for single user transmissions, was shown to be a sub-optimal implementation of Dirty Paper Coding (DPC) [14], and to achieve transmission at the full channel capacity [15]. The dynamic range of the precoded waveform increases in the presence of deep channel fades. To overcome this problem THP is implemented with a modulo operator. Since the operation of THP is tightly connected to the modulated signal constellation, the implementation of THP in the context of SC-FDMA is difficult since the SC-FDMA signal does not have a distinct constellation in the time-domain as

978-1-4244-2517-4/09/$20.00 ©2009 IEEE

a result of oversampling. For this reason a novel frequency-domain implementation of THP is considered in this paper.

This paper is organized as follows. In section II the SC-FDMA transmission model is given. Sections III and IV provide an overview of the time-domain and the novel frequency-domain implementations of THP. Section V presents a comparison between the Complementary Cumulative Density Function (CCDF) of the PAPR for each scheme as well as their BER performance. Conclusions are presented in section VI.

II. SC-FDMA Transmission in Multipath Channels

The 3GPP LTE group, [16]- [17], is developing the next generation of mobile communication standards [17]. A working assumption for 3GPP LTE is the use of SC-FDMA on the uplink. The principle of SC-FDMA signaling is presented in [16]- [18]. Fig. 1 shows the structure of the uplink SC-FDMA system considered in this paper. The variables in Fig. 1 are defined later in the paper. For the i-th user, and for each block of M data samples, $\mathbf{x}^{(i)} = \left[x_0^{(i)}, x_1^{(i)}, \cdots, x_{M-1}^{(i)}\right]^{\mathcal{T}}$, the transmitter maps the corresponding M frequency components of the block, $\mathbf{X}^{(i)} = \left[X_0^{(i)}, X_1^{(i)}, \cdots, X_{M-1}^{(i)}\right]^{\mathcal{T}}$, resulting from an $M-$point DFT of the data samples, onto a set of M active sub-carriers selected from a total of $N = QM$ sub-carriers ($Q > 1$). The remaining $N - M$ sub-carriers are inactive since they are used by other uplink users.

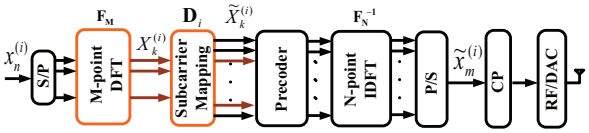

Fig. 1. Transmitter structure for SC-FDMA.

Here we consider distributed and localized SC-FDMA (D-FDMA and L-FDMA respectively) [16]. We denote the sub-carrier mapping transform matrix for the i-th user by $\mathbf{D}_i$. The entries of this matrix for both D-FDMA and L-FDMA are given in Equations (1) and (2) respectively:

$$\mathbf{D}_i = \left[\mathbf{0}_{(s_i-1)M\times M};\ \left(\mathbf{u}_i^M\right)^{\mathcal{T}};\mathbf{0}_{Q'\times M};\left(\mathbf{u}_{i+Q'}^M\right)^{\mathcal{T}};\right.$$
$$\left.\cdots;\mathbf{u}_{i+MQ'}^{\mathcal{T}};\mathbf{0}_{(Q-Q')M\times M}\right] \quad (1)$$

$$\mathbf{D}_i = \left[\mathbf{0}_{(i-1)M\times M};\mathbf{I}_M;\mathbf{0}_{(Q-i)M\times M}\right] \quad (2)$$

where the generic $\mathbf{I}_K$ and $\mathbf{0}_{L\times K}$ matrices denote, respectively, the $K \times K$ identity matrix, and the $L \times K$ all-zeros matrix. $\mathbf{u}_k^K$ denotes the unit column vector, of length K, with all zero entries except at k. s_i and Q' denote the start of the i-th user's sub-carriers and the sub-carrier spacing for D-FDMA. We denote Ψ_i as the set of sub-carriers occupied by the i-th user. Since the columns in both mapping matrices are orthogonal, the demapping matrix is $\mathbf{D}_i^{\mathcal{T}}$ since the mapping matrix satisfies:

$$\mathbf{D}_j^{\mathcal{T}}\mathbf{D}_i = \begin{cases} \mathbf{I}_M & j = i \\ \mathbf{0}_{M\times M} & j \neq i \end{cases} \quad (3)$$

Fig. 2 illustrates the distributed and localized sub-carrier mapping modes for an uplink transmission system with four resource units. The sub-carrier mapping produces $\widetilde{\mathbf{X}}^{(i)} = \mathbf{D}_i\mathbf{X}^{(i)}$ such that $\widetilde{\mathbf{x}}^{(i)} = \left[\widetilde{X}_0^{(i)}, \widetilde{X}_1^{(i)}, \cdots, \widetilde{X}_{N-1}^{(i)}\right]^{\mathcal{T}}$. $\widetilde{\mathbf{X}}^{(i)}$ is processed by the N-point Inverse DFT (IDFT) to produce the time-domain

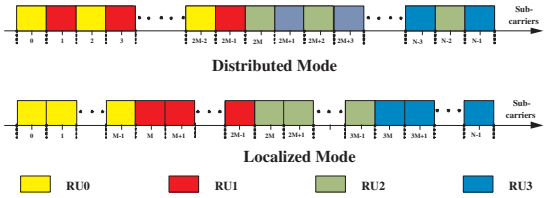

Fig. 2. Transmitter structure for SC-FDMA

transmitted signal $\widetilde{\mathbf{x}}^{(i)} = \left[\widetilde{x}_0^{(i)}, \widetilde{x}_1^{(i)}, \cdots, \widetilde{x}_{N-1}^{(i)}\right]^{\mathcal{T}}$.

Prior to transmission a cyclic prefix (CP) of length P is inserted into each transmitted block. Although this is performed at the expense of transmission bandwidth, the CP prevents interference from previously transmitted blocks due to multipath propagation, and hence maintains orthogonality between the sub-carriers.

Table I shows the main simulation parameters used in this paper. We assume that the total number of sub-carriers N is 512 and that each user has access to 128 sub-carriers with a spreading factor Q of 4. We assume the use of Urban LoS scenarios Range1 (LoS1) and Range2 B5b (LoS2) as well as Urban NLoS scenario C3 as defined in [19].

Carrier Frequency	2 GHz
Transmission Bandwidth	5 MHz
Total Number of Sub-carriers (N)	512
Number of Sub-carriers per User (M)	128
Guard Interval (P)	64
SC-FDMA Symbol Duration (μ)	150μs
Channel Knowledge	Perfect
Fading per tap	i.i.d. Rayleigh
Channel Coding	Not included
Signal Constellation	QPSK
Delay Profile	Model Dependent [19]

TABLE I
SC-FDMA Simulation Parameters

The SC-FDMA transmitted signal can be represented by:

$$\widetilde{\mathbf{x}}^{(i)} = \mathbf{C}\mathbf{F}_N^{-1}\mathbf{D}_i\mathbf{F}_M\mathbf{x}^{(i)} \quad (4)$$

where $\mathbf{F}_N^{-1}$ and $\mathbf{F}_M$ are the N-point IDFT and M-point DFT matrix respectively. The generic K-point DFT matrix has entries $[\mathbf{F}_K]_{p,q} = e^{-j2\pi\frac{pq}{K}}$, and its inverse is $\mathbf{F}_K^{-1} = \mathbf{F}_K^{\mathcal{H}}$, where $(\bullet)^{\mathcal{H}}$ denotes the *Hermitian* transpose. $\mathbf{C}$ represents the CP insertion matrix:

$$\mathbf{C} = [\mathbf{CP}, \mathbf{I}_N]^{\mathcal{T}}, \quad \mathbf{CP} = \left[\mathbf{0}_{P\times(N-P)}, \mathbf{I}_P\right]^{\mathcal{T}}$$

The received signal $r_n^{(i)}$ at time t, for the SC-FDMA system operating in a multipath fading channel corrupted by Additive White Gaussian Noise, $w_n^{(i)}$, with variance σ_n^2 is given by:

$$r_n^{(i)} = \sum_{k=0}^{L} h_k\widetilde{x}_{n-k}^{(i)} + w_n^{(i)} = \mathbf{h}^{\mathcal{T}}\widetilde{\mathbf{x}}_{n:n-L}^{(i)} + w_n^{(i)} \quad (5)$$

where the Channel Impulse Response (CIR) of length L is $\mathbf{h} = [h_0, h_1, \cdots, h_L]^{\mathcal{T}}$, and $\widetilde{\mathbf{x}}_{n:n-L}^{(i)} = \left[\widetilde{x}_n^{(i)}, \widetilde{x}_{n-1}^{(i)}, \cdots, \widetilde{x}_{n-L}^{(i)}\right]^{\mathcal{T}}$. This means, after removing the CP at the receiver, the received signal $\mathbf{r}^{(i)} = \left[r_0^{(i)}, r_1^{(i)}, \cdots, r_{N-1}^{(i)}\right]$ can be described as:

$$\mathbf{r}^{(i)} = \mathbf{H}\widetilde{\mathbf{x}}^{(i)} + \mathbf{w}^{(i)} = \mathbf{F}_N^{-1}\overline{\mathbf{H}}\mathbf{F}_N\widetilde{\mathbf{x}}^{(i)} + \mathbf{w}^{(i)} \quad (6)$$

where $\mathbf{H}$ is a circulant channel matrix, $\mathbf{w}$ is a column vector containing complex AWGN noise samples, and $\overline{\mathbf{H}}$ is a diagonal matrix, whose entries are generated from the N-point DFT of the channel impulse response.

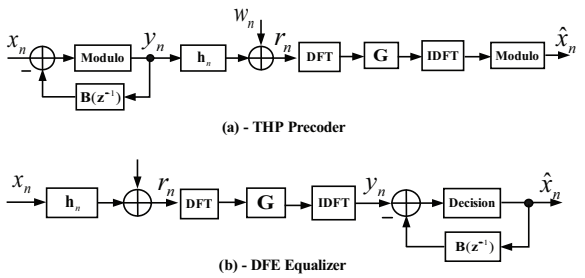

Fig. 3. THP Precoder and DFE Equalizer structure

III. Frequency-Domain THP

THP is an effective way to account for the error propagation problem in the DFE, since the feedback filter can be implemented at the transmitter. Here we consider the Tomlinson-Harashima precoder combined with single-carrier Frequency-Domain Equalization (SC-FDE) for uplink SC-FDMA. We denote this scheme as THP-FDE. The structure of the THP-FDE is shown in Fig. 3. The operation of the TH-Precoder is described in [9]- [10]. The THP-FDE consists of an L-order feedback filter, $\mathbf{B}(z^{-1})$, and a modulo operator at the transmitter and an N tap frequency-domain equalizer at the receiver with weights G_k. The transfer function of the THP, $\mathbf{B}(z^{-1})$, is given by $\mathbf{B}(z^{-1}) = \sum_{n=1}^{L} b_n z^{-n}$, where b_n are the precoder's coefficients.

As a result of precoding the dynamic range of the precoded waveform increases, especially for channels experiencing deep fades. This increases the PAPR of the transmitted waveform. In order to overcome this limitation the THP is implemented with a modulo device. The modulo operation aims to reduce the dynamic range of the precoded waveform, regardless of the precoder's coefficients. For an $\mathcal{M}^2$-QAM constellation, the output of the modulo operation is:

$$x_n = z_n - 2\mathcal{M}\left\lfloor \frac{\Re(z_n)}{2\mathcal{M}} + \frac{1}{2} \right\rfloor - j2\mathcal{M}\left\lfloor \frac{\Im(z_n)}{2\mathcal{M}} + \frac{1}{2} \right\rfloor \quad (7)$$

where $\Re(\bullet)$ and $\Im(\bullet)$ denote the real and imaginary parts respectively. $\lfloor \bullet \rfloor$ denotes the flooring operation. z_n, the input of the modulo device, as shown in Fig. 3, is related to the precoder's output by:

$$y_n = x_n - \sum_{m=1}^{L} b_m y_{n-m} \quad (8)$$

where the $\mathcal{M}^2$-QAM symbol x_n is the precoder's input. If we re-arrange both sides of equation (8) and take the N-point DFT of both sides of this equation we obtain:

$$X_k = \left(1 + \sum_{n=1}^{L} b_n e^{-j2\pi \frac{kn}{N}}\right) Y_k = B_k Y_k \quad (9)$$

where $B_k = \left(1 + \sum_{n=1}^{L} b_n e^{-j2\pi \frac{kn}{N}}\right)$.

Since the operation of THP is tightly connected to the signal constellation, the implementation of THP in the context of SC-FDMA becomes difficult since the SC-FDMA does not have a distinct constellation. This is due to oversampling in the time-domain, which means that only 1 in Q, and 1 in Q', samples fall on the transmit constellation for localized (L-FDMA) and distributed (D-FDMA) SC-FDMA, respectively. In addition, the majority of previous precoding work relies on time-domain filtering of the data samples. As the delay spread of the channel increases, the implementation of the precoder requires greater computational complexity. For these reasons we present a realizable and effective frequency-domain implementation of THP.

If the precoder's input is the SC-FDMA modulated signal, $\widetilde{\mathbf{x}}$ after CP insertion, then by ignoring the first P samples the precoder's output $\mathbf{y}$ can be expressed in matrix form as:

$$\widetilde{\mathbf{x}} = \begin{bmatrix} 1 & 0 & \cdots & 0 & b_L & \cdots & b_1 \\ b_1 & \ddots & \ddots & \vdots & \ddots & \ddots & \vdots \\ \vdots & \ddots & 1 & 0 & \cdots & 0 & b_L \\ b_L & \cdots & b_1 & 1 & 0 & \cdots & 0 \\ 0 & \ddots & \vdots & b_1 & 1 & \ddots & \vdots \\ \vdots & \ddots & b_L & \vdots & \ddots & \ddots & 0 \\ 0 & \cdots & 0 & b_L & \cdots & b_1 & 1 \end{bmatrix} \mathbf{y} = \overline{\mathbf{B}}\mathbf{y} \quad (10)$$

Combining equations (4) and (10), and ignoring $\mathbf{C}$, leads to:

$$\mathbf{y} = \overline{\mathbf{B}}^{-1}\widetilde{\mathbf{x}} = \mathbf{P}\widetilde{\mathbf{x}} \quad (11)$$

$$= \left(\mathbf{F}_N^{-1}\mathbf{\Pi}\mathbf{F}_N\right)\mathbf{F}_N^{-1}\mathbf{D}_i\mathbf{F}_M\mathbf{x} = \mathbf{F}_N^{-1}\mathbf{\Pi}\mathbf{D}_i\mathbf{F}_M\mathbf{x} \quad (12)$$

where $\mathbf{P}$ is the precoding matrix. Since the inverse of a circulant matrix is a circulant matrix, the pre- and post-multiplication of $\mathbf{P}$ by the N-point DFT and IDFT matrices, respectively, produces $\mathbf{\Pi}$, a diagonal matrix containing the eigenvalues of $\mathbf{P}$, which are the DFT of the first row $\mathbf{P}$. This means that the implementation of the transmit precoder can be moved from the time-domain to the frequency-domain. This reduces the NL complex multiplications and the NL complex additions performed in the time-domain implementation of the precoder to only M multiplications in the frequency-domain, which translates to reduced complexity.

IV. THP Coefficients

The output of THP-FDE is given by:

$$\widehat{x}_n = \frac{1}{M}\sum_{k\in\Psi_i} G_k R_k e^{j2\pi\frac{kn}{M}} \quad (13)$$

$$= \frac{1}{M}\sum_{k\in\Psi_i} G_k\left(H_k Y_k + W_k\right) e^{j2\pi\frac{kn}{M}} \quad (14)$$

$$= \frac{1}{M}\sum_{k\in\Psi_i} G_k H_k Y_k e^{j2\pi\frac{kn}{M}} + + \widetilde{w}_n \quad (15)$$

where the k-th sub-carrier of the frequency-domain equalizer weights, the received signal and the additive noise, are denoted by G_k, R_k and W_k respectively. $\widetilde{w}_n$ is the filtered noise at the output of the FDE. Combining equations (9) and (15) produces:

$$\widehat{x}_n = \frac{1}{M}\sum_{k\in\Psi_i}\left[\left(G_k H_k - B_k\right) Y_k + X_k\right] e^{j2\pi\frac{kn}{M}} + \widetilde{w}_n$$

$$= x_n + \underbrace{\frac{1}{M}\sum_{k\in\Psi_i}\left(G_k H_k - B_k\right) Y_k e^{j2\pi\frac{kn}{M}}}_{=v_n} + \widetilde{w}_n \quad (16)$$

The error sequence of the THP-FDE, $e_n = \widehat{x}_n - \widetilde{x}_n$ where v_n is the residual interference in the current symbol decision. This shows that the output of the FDE is composed of the filtered noise $\widetilde{w}_n$ from the FDE, and the residual interference as a result of the precoder ($e_n = v_n + \widetilde{w}_n$), which is demonstrated in Fig. 4.

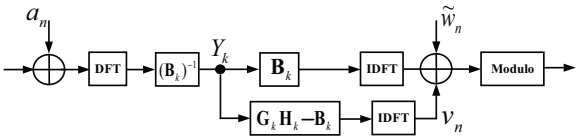

Fig. 4. Equivalent THP Precoder structure

A. Zero-Forcing THP-FDE

The impulse response of the cascade of the discrete-time channel impulse response and the feedforward equalizer is the M-point IDFT of the product of H_k and G_k, as shown in equation (16), i.e.

$$u_n = \frac{1}{N}\sum_{k=1}^{N}\left(G_k H_k\right) e^{j2\pi\frac{kn}{N}}, \qquad n = 0, \cdots, L \tag{17}$$

Under the Zero Forcing (ZF) criterion, from [20] and [21], all interference must be cancelled by the THP. As a result, the precoder's coefficients under the ZF criterion must be chosen such that $b_n = u_n$. From equation (17), the coefficients of the FDE must satisfy:

$$G_k = \frac{1}{H_k}\sum_{n=0}^{L} u_n e^{-j2\pi\frac{kn}{N}} = \frac{1}{H_k}\left(1 + \sum_{n=1}^{L} b_n e^{-j2\pi\frac{kn}{N}}\right) \tag{18}$$

This means that the coefficients u_n can be chosen freely, which leads to computing the coefficients G_k and b_n. Here we choose the coefficient G_k such that the power of the filtered noise is minimized. Under this condition, the cost function of the ZF THP-FDE is given by:

$$J_{\text{ZF}} = \frac{\sigma_n^2}{M}\sum_{k\in\Psi_i}|G_k|^2 = \frac{\sigma_n^2}{M}\sum_{k\in\Psi_i}\left|\frac{1}{H_k}\left(1 + \sum_{n=1}^{L} b_n e^{-j2\pi\frac{kn}{N}}\right)\right|^2 \tag{19}$$

Let $\mathbf{b} = [b_1, \cdots, b_L]^{\mathcal{T}}$. From [21], the precoder's coefficients satisfy[1] $\mathbf{Ab} = -\mathbf{a}$, where:

$$[\mathbf{A}]_{m,l} = \sum_{k=0}^{N-1}\frac{e^{-j2\pi\frac{k(l-m)}{N}}}{\left|\overline{\mathbf{H}}_{k,k}\right|^2}, \quad [\mathbf{a}]_m = \sum_{k=0}^{N-1}\frac{e^{-j2\pi\frac{km}{N}}}{\left|\overline{\mathbf{H}}_{k,k}\right|^2}$$

where $\overline{\mathbf{H}}_{k,k}$ represents the k-th entry on the diagonal of $\overline{\mathbf{H}}$. with $1 \le m, l \le L$

B. Minimum Mean Square Error THP-FDE

Under the MMSE criterion the coefficients of the FDE and precoder are chosen such that the sum of the power of the filtered noise, and the power of the residual interference are minimized. The cost function of the THP-FDE under the MMSE criterion is:

$$J_{\text{MMSE}} = \mathbf{E}\left[\|e_n\|^2\right] = \mathbf{E}\left[\left(v_n + \widetilde{w}_n\right)\left(v_n + \widetilde{w}_n\right)^{\mathcal{H}}\right] \tag{20}$$

[1]In [21], the feedback filter coefficients are b_k, whereas here these were assumed to be $-b_k$, hence the use of $\mathbf{Ab} = -\mathbf{a}$ rather than $\mathbf{Ab} = \mathbf{a}$.

where σ_s^2 denotes the power of the signal x_n. $\mathbf{E}[\bullet]$ denotes the expectation operator. Under the orthogonality principle, the precoder's output and the noise samples are uncorrelated and therefore $\mathbf{E}\left[v_n\widetilde{w}_n^{\mathcal{H}}\right] = 0$. This means that equation (20) can be simplified to:

$$J_{\text{MMSE}} = \frac{1}{M}\sum_{k\in\Psi_i}\left[\sigma_n^2|G_k|^2 + \sigma_s^2|G_k H_k - B_k|^2\right] \tag{21}$$

As shown in [21], the FDE coefficient satisfy:

$$G_k = \frac{H_k^* B_k}{|H_k|^2 + \frac{\sigma_n^2}{\sigma_s^2}} \tag{22}$$

Combining equations (22) and (21) produces:

$$J_{\text{MMSE}} = \frac{\sigma_n^2}{M}\sum_{k\in\Psi_i}\frac{1}{|H_k|^2 + \frac{\sigma_n^2}{\sigma_s^2}}\left|1 + \sum_{n=1}^{L} b_n e^{-j2\pi\frac{kn}{N}}\right|^2 \tag{23}$$

The time-domain THP filter coefficients therefore satisfy $\mathbf{Ab} = -\mathbf{a}$, where:

$$[\mathbf{A}]_{m,l} = \sum_{k=0}^{N-1}\frac{e^{-j2\pi\frac{k(l-m)}{N}}}{\left|\overline{\mathbf{H}}_{k,k}\right|^2 + \frac{\sigma_n^2}{\sigma_s^2}}, \quad [\mathbf{a}]_m = \sum_{k=0}^{N-1}\frac{e^{-j2\pi\frac{km}{N}}}{\left|\overline{\mathbf{H}}_{k,k}\right|^2 + \frac{\sigma_n^2}{\sigma_s^2}}$$

with $1 \le m, l \le L$.

V. Results And Discussion

Throughout this section we assume that channel estimation is performed at the base-station, where the mean of the wideband channel is normalized to unity and the channel information is sent back to the mobile unit. This means that transmit precoding cannot compensate for fluctuations in the channel mean power. In other words, precoding is only concerned with flattening the channel and does not necessarily perform fast power control. For instance, in a narrowband channel precoding would play no role at the transmitter.

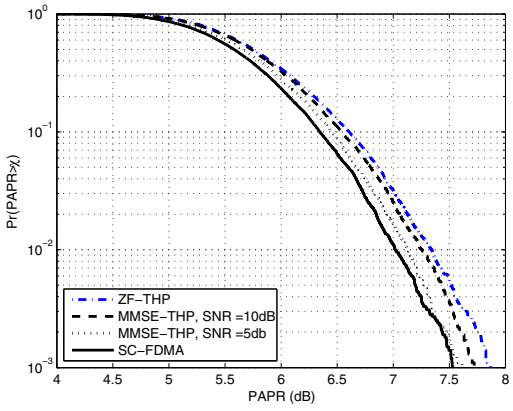

Fig. 5. PAPR Characteristics of ZF and MMSE THP Precoded SC-FDMA

Fig. 5 shows the CCDF of the PAPR for the ZF and MMSE THP waveforms. As can be seen, the PAPR of the ZF-THP is higher than the PAPR of the MMSE-THP, which in turn reduces as the noise variance increases (equivalently as the SNR decreases). This difference in PAPR characteristic between the two schemes is due to the difference in the dynamic range of the precoders' magnitudes. That is, for the ZF-THP, as a result of the high dynamic range of the

precoder's magnitudes, the dynamic range of the precoded SC-FDMA waveform becomes higher than the standard SC-FDMA waveform. The precoded waveform therefore has a high PAPR. Similarly, for the MMSE-THP, the decreasing PAPR of the MMSE-THP waveform as the SNR decreases can be explained by the fact that the dynamic range of the precoder's magnitudes reduce by increasing the noise variance.

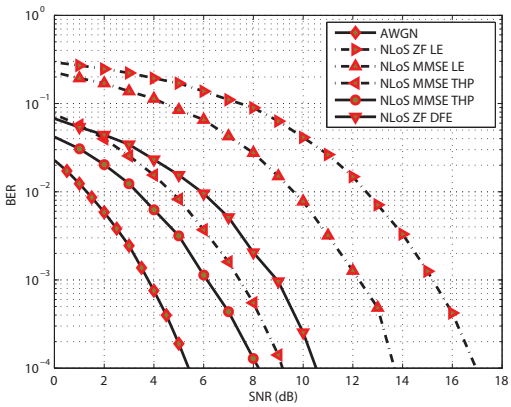

Fig. 6. BER performance of the ZF and MMSE THP for the LoS2 Channel scenario compared to the BER performance of MMSE DFE, MMSE LE, ZF LE and AWGN

Fig. 6 shows the BER performance of the different equalizers and precoders. The results were obtained using the same system settings described in Table I and assuming L-FDMA uplink transmission and perfect channel knowledge at the transmitter. The BER performance was obtained for the NLoS C3 model. The ZF based linear equalizer offers the worst BER performance when compared to the other schemes. This is due to the noise enhancement resulting from the channel inversion applied by the ZF. The MMSE LE offers an optimum solution under the MMSE criterion and its performance is superior to that of the ZF LE as it takes into account the presence of noise at the receiver front-end. As mentioned earlier, the DFE offers a better BER performance compared to the LE. Its performance is however inferior to that of the MMSE THP with joint FDE. This is explained by the degradation that results from the error propagation problem in the feedback filter. Furthermore, the MMSE-THP offers a better BER performance compared to the ZF-THP since the MMSE-THP reduces the magnitude of the error resulting from both the residual ISI, as a result of the combined channel and FDE, and the filtered additive noise, contrary to the ZF-THP, which only cancels the residual ISI.

VI. Conclusion

In this paper we have presented a frequency-domain implementation of THP for uplink SC-FDMA transmission. The frequency-domain THP is a low complexity implementation of the THP that can be applied to different systems regardless of the signal constellation. Here we proposed the frequency-domain THP for SC-FDMA and both the ZF and MMSE THP designs were considered. The MMSE-THP offers a better BER performance compared to the ZF-THP, and also has a lower PAPR.

Although precoding achieves a superior performance compared to frequency domain equalization, the implementation of transmit precoding requires perfect knowledge of the uplink channel, with no latency. Further work is required to address how channel estimation and tracking can assist the precoder in the case of mobility, channel estimation error and channel mismatch.

Acknowledgment

The authors would like to thank the Algerian Government for their financial support of this PhD, and the Centre for Communications Research for the provision of research facilities and access to a computing cluster.

References

[1] R. van Nee, and R. Prasad, "OFDM for Wireless Multimedia Communications", Norwood, MA: Artech House, 2000.
[2] H. Yin, and S. Alamouti, "OFDMA: A Broadband Wireless Access Technology", IEEE Sarnoff Symposium, pp. 1–4, 27-28 March 2006
[3] 3GPP, "Technical Specification Group Radio Access Networks Physical layer aspects for evolved Universal Terrestrial Radio Access (UTRA)", 3GPP, Technical Specification TR 25.814 V7.1.0 Sep. 2006, Release 7
[4] David Falconer, S. Lek Ariyavisitakul, Anader Benyamin-Seeyar, Brian Eidson, "Frequency Domain Equalization for Single-Carrier Broadband Wireless Systems", Communications Magazine, IEEE, Apr. 2002
[5] G. Berardinelli, B. E. Priyanto, T. B. Srensen, and P. Mogensen, "Improving SC-FDMA Performance by Turbo Equalization in UTRA LTE Uplink," IEEE Vehicular Technology Conference (VTC) 2008 Spring, Marina Bay, Singapore, May 2008
[6] N. Benvenuto and S. Tomasin, "Block iterative DFE for single carrier modulation", Electronics Letters, pp. 1144-1145, vol. 38, No. 19, September 2002.
[7] M.V. Eyuboglu, "Detection of coded modulation signals on linear, severely distorted channels using decision feedback noise prediction with interleaving", IEEE Trans. Commun. 36 (4) (April 1988) 401-409.
[8] Y. Zhu and K. B. Letaief, "Single carrier frequency-domain equalization with noise prediction for broadband wireless systems," in Proc. of IEEE Globecom'04, vol.5, Dec. 2004
[9] M. Tomlinson, "New automatic equalizer employing modulo arithmetic," Electron. Lett., vol. 7, pp. 138-139, Mar. 1971.
[10] H. Harashima and H. Miyakawa, "Matched-transmission technique for channels with intersymbol interference,"' IEEE Trans. Commun., vol. 20, pp. 774-780, Aug. 1972.
[11] M. Vedat Eyuboglu, G. David Forney, "Trellis Precoding: Combined Coding, Precoding and Shaping for Intersymbol Interference Channels", IEEE Trans. Inform. Theory, vol. 38, No.2, pp. 301-314, Mar. 1992
[12] R. Laroia, S. Tretter and N. Farvardin, "A Simple and Effective Precoding Scheme for Noise Whitening on Intersymbol Interference Channels", IEEE Trans. on Communications, October 1993.
[13] Lee-Fang Wei: "Precoding Technique for Partial-Response Channels with Applications to HDTV Transmission", IEEE Journal on Selected Areas in Communications 11(1): 127-135 (1993)
[14] C. B. Peel, "On "dirty-paper-coding"," IEEE Signal Processing Magazine, vol. 20, no 3, pp 112–113, May 2003
[15] Richard D. Wesel, John M. Cioffi: "Achievable Rates for Tomlinson-Harashima Precoding". IEEE Transactions on Information Theory 44(2): 824-831 (1998)
[16] Hyung G. Myung, "Single Carrier Orthogonal Multiple Access Technique for Broadband Wireless Communication", Polytechnic University, January 2007
[17] Hyung G. Myung, "Technical Overview of 3GPP Long Term Evolution (LTE)",http://hgmyung.googlepages.com/3gppLTE.pdf, Feb.8, 2007
[18] Hyung G. Myung, Junsung Lim, and David J.Goodman, "Single Carrier FDMA for Uplink Wireless Transmission", 2006 IEEE Vehicular Technology Magazine 1 September 2006
[19] Final report on link level and system level channel Models, IST–2003–507581 WINNER D5.4 ver 1.4
[20] R.D. Wesel, J.M. Cioffi, "Precoding and the MMSE-DFE", Proceedings of the 28th Asilomar Conference on Signals, Systems & Computers, 1995.
[21] N. Benvenuto and S. Tomasin, "On the Comparison between OFDM and Single-Carrier Modulation with a DFE Using a Frequency-Domain Feedforward Filter," IEEE Trans. Commun., vol. 50, no. 6, pp. 947-955, Jun. 2002.